Photoinduced anisotropy of IWK-2D azobenzene molecular glassy films

Andris Ozols[a *], Edvins Letko[b], Peteris Augustovs[c], Dmitry Saharov[d], Elmars Zarins[e] and Valdis Kokars[f]

Faculty of Material Science and Applied Chemistry, Riga Technical University, Paula Valdena iela 3/7, LV-1007, Riga, Latvia

[a] Andris.Ozols@rtu.lv, [b] edvin1234@inbox.lv, [c] peterisaug@gmail.com, [d] Dmitry.Saharov@gmail.com, [e] Elmars.Zarins@rtu.lv, [f] Valdis.Kokars@rtu.lv

Keywords: photoinduced anisotropy, polarization holographic gratings, surface relief gratings, azobenzene molecular glasses.

Abstract. We have experimentally studied photoinduced anisotropy (PA) of holographic gratings in IWK-2D [precise chemical notation: 2-(3-(4-((4-(bis (2-(trityloxy) ethyl)amino)phenyl)diazenyl)styryl)-5,5-dimethylcyclohex-2-enylidene) malononitrile] azobenzene molecular glassy films in transmission and reflection modes using a special simultaneous holographic recording and readout setups which enabled measurements of PA time evolution. PA manifested itself by diffraction efficiency difference with linear *s*- and *p*-polarizations. Three different types of polarization holographic gratings were recorded and studied using *p-p, L-L* and *L-R* polarized beams creating different recording interference patterns. Atomic force microscope (AFM) was used to study the surface profile changes. Experimental evidence was obtained that the transmission mode PA was due to the both recorded surface relief and volume polarization gratings whereas the reflection mode PA was due to the recorded surface relief gratings. The main PA features were similar for all three types of polarization gratings whereas details were different. PA properties of IWK-2D films were notably distinctive from those of previously studied films.

Introduction

Photoinduced anisotropy (PA) was discovered by F.Weigert in 1919 when he observed photoinduced linear dichroism and birefringence in silver halide films [1]. Generally, by PA one means the effect of elliptical dichroism and birefringence induced by polarized light in an initially isotropic sample thus allowing also for possible photoinduced gyrotropy. PA of a material enables the polarization hologram recording. In the same time, polarization holograms carry information about PA processes in the materials.

Azobenzene organic materials exhibiting PA and enabling also surface relief grating (SRG) formation due to *trans-cis-trans* photoisomerization and athermal photofluidization [2-4] have found numerous applications in optoelectronics including holographic information recording [3,4]. In the recent years, azobenzene molecular glassy films have attached attention in this respect [5, 6]. Therefore, PA studies are of interest. Previously we have holographically studied PA in molecular glassy films containing diphenylamine azochromophores [7] using only *p-p* recording to induce PA. This paper is devoted to holographic studies of PA in triphenyl group containing molecular glassy films of azobenzene with additionally incorporated 5,5-dimethylcyclohex-2-enylidene structural fragments and dicyanomethylene electron acceptor moieties (denoted as IWK-2D) using *p-p, L-L* and *L-R* recording beam polarizations. The obtained results are quite different compared to the previous ones [7].

Experiments and results

IWK-2D [2-(3-(4-((4-(bis (2-(trityloxy) ethyl)amino)phenyl)diazenyl)styryl)-5,5-dimethyl cyclohex-2-enylidene) malononitrile] azobenzene molecular glassy film synthesized and

characterized by Elmars Zarins and Valdis Kokars in our Faculty was studied in our experiments. Its structural formula is shown in Fig.1. Film was spin-coated onto the glass substrate and its thickness was about 3 μm. Absorption coefficients (α) were 4.06 μm^{-1} and 0.423 μm^{-1} at 532 and 632.8 nm , respectively.

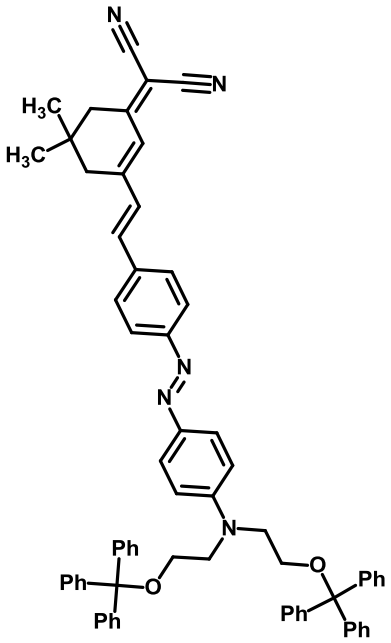

Fig.1. Chemical structural formula of IWK-2D film. It has *trans*-absorption maximum at 500 nm and glass transition temperature T_q =105^0 C.

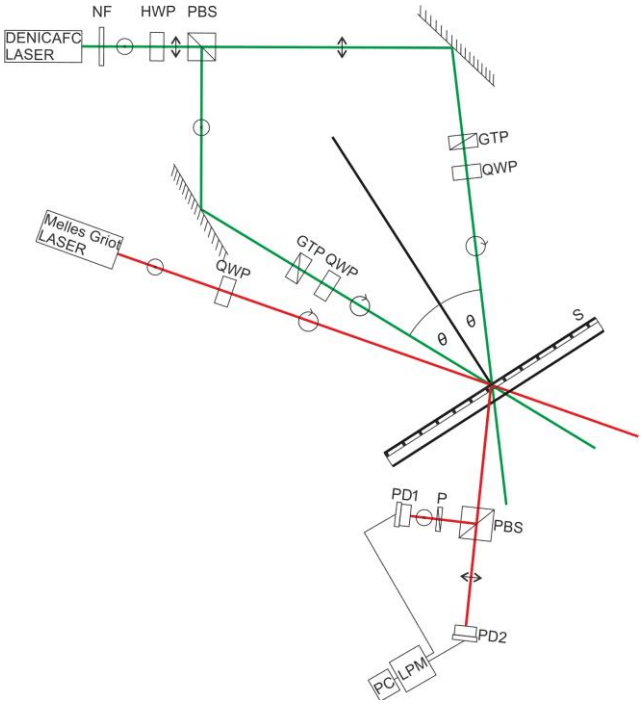

Fig.2. Experimental setup for transmission mode PA measurements. Notations are explained in the text.

Experimental setups for PA measurements in transmission and reflection mode in the case of *L*-*L* recording polarizations are shown in Figs. 2 and 3. The following notations are used: NF-neutral filter, HWP-half-wave plate, PBS-polarization beam splitter, QWP-quarter-wave plate, GTP-Glass-Thompson polarizer, S-sample, PD1 and PD2-photodetectors, P-polarizer, LPM-laser power meter, PC-personal computer. In the case of other polarizations setups were similar except for different polarization forming elements in recordings beams before the sample. Two 532 nm symmetrically incident KLASTECH DENICAFC 532-300 diode pumped 9.5 mW laser beams with a total intensity I=0.75 W/cm^2 were used for holographic grating recording with the period of 2 μm. One circularly polarized 1 mW 632.8 nm laser beam from Melles Griot 25LH928-230 He-Ne gas laser was used for holographic grating readout. PBS after the sample allowed for simultaneous real-time readout of diffraction efficiencies (DE) with *s*- (η_s) and *p*-polarizations (η_p). "Ophir Laserstar" laser power meter enabled the measurement and recording of diffracted light powers.

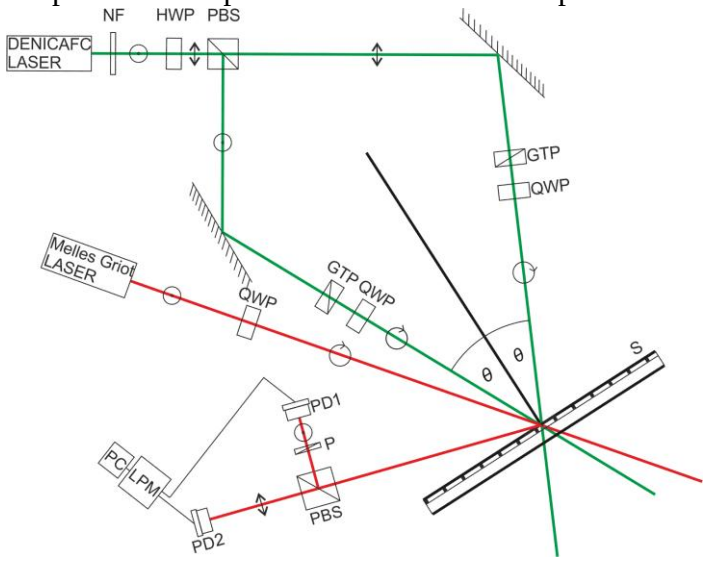

Fig.3. Experimental setup for reflection mode PA measurements. Notations are explained in the text.

In our experiments, DE was defined as the ratio of diffracted beam power to the incident readout beam power. Recording efficiency was also described by specific recording energy $W=It/\eta$ [J/cm^2%] where t was exposure time. To characterize PA we have introduced two quantities- the DE difference $\eta_s - \eta_p$ and PA contrast $A=(\eta_s - \eta_p)/(\eta_s + \eta_p)$. This quantity changes from -1 to +1. In both cases the anisotropy is maximal. The measurement errors did not exceed 2.5% for DE, 3.1% for W, 15% for $\eta_s - \eta_p$ and A on transmission, and 9.8% for $\eta_s - \eta_p$ and A on reflection. The results were corrected for a slight difference of photodetector sensitivity. Experimental results are presented in Figs.4-15 and Tables 1-2. Three curves in each figure correspond to three repeated measurements at adjacent sites of the sample.

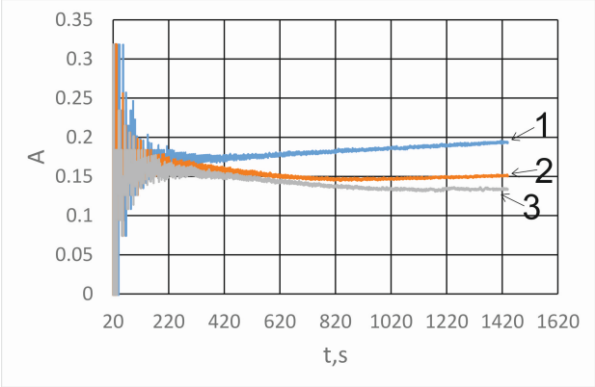

Fig.4. PA contrast versus time in the case of *L-L* recording. Transmission mode.

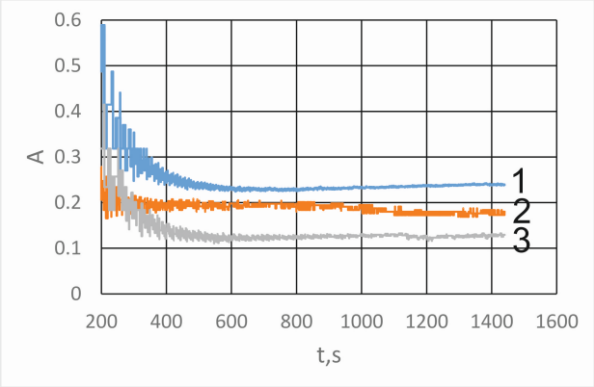

Fig.5. PA contrast versus time in the case of *L-L* recording. Reflection mode.

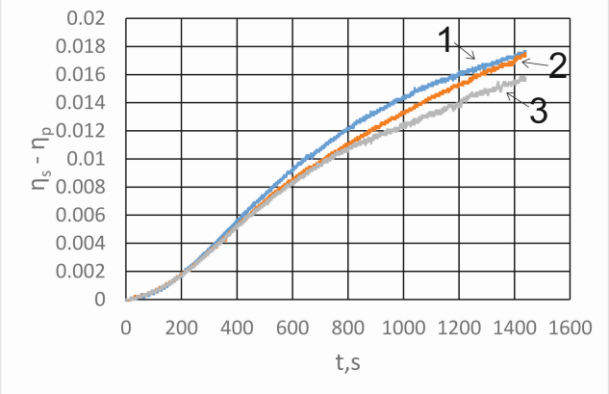

Fig.6. DE difference versus time in the case of *L-L* recording. Transmission mode.

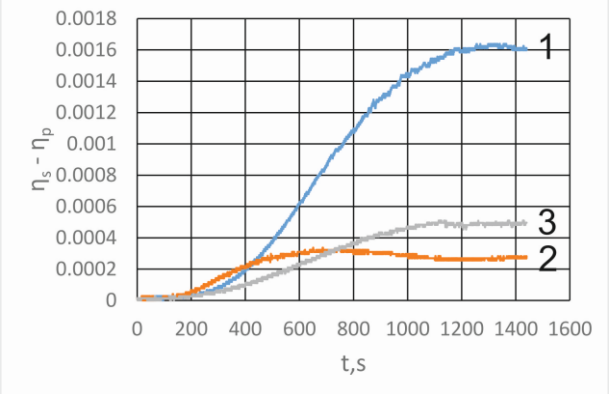

Fig.7. DE difference versus time in the case of *L-L* recording. Reflection mode.

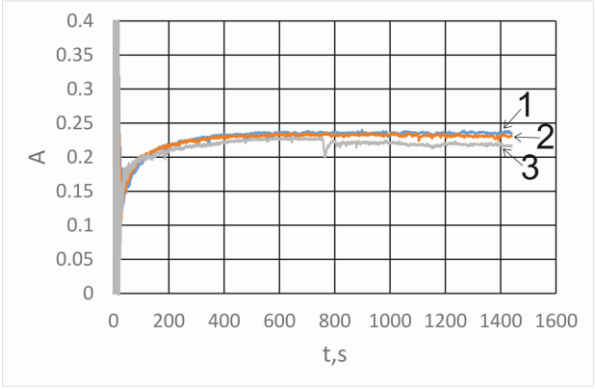

Fig.8. PA contrast versus time in the case of *L-R* recording. Transmission mode.

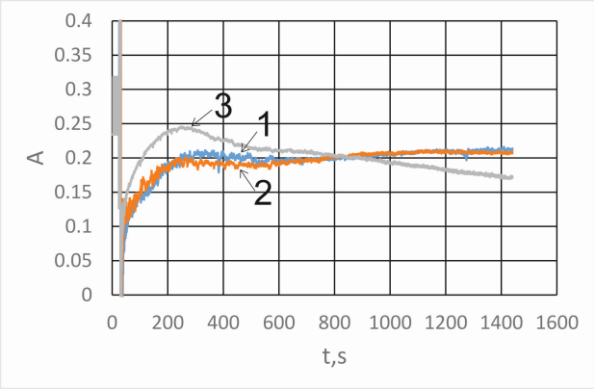

Fig.9. PA contrast versus time in the case of *L-R* recording. Reflection mode.

Figs.4-15 show that time varying PA has taken place in all cases. It can be seen from these figures that the main features of PA were similar in all corresponding cases. However, more detailed consideration reveals the qualitative distinction of *A* curves in the case of *L-L* recording from other cases, and DE difference curve distinction on transmission and reflection in all cases. *A* curves in the *L-L* case start from positive values whereas they start with negative *A* values in other cases. DE difference curves display maxima on reflection, but not on transmission thus showing difference of PA on transmission and reflection.

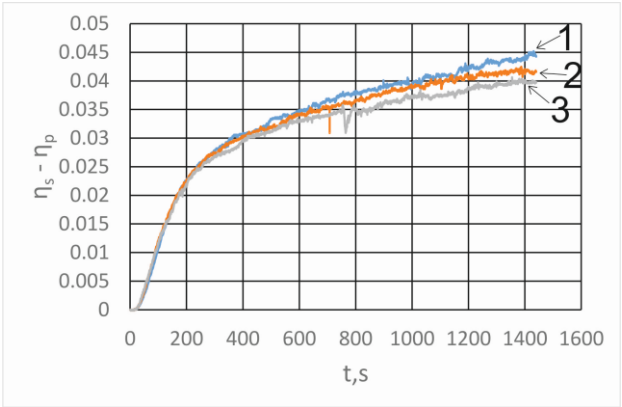

Fig.10. DE difference versus time in the case of *L-R* recording. Transmission mode.

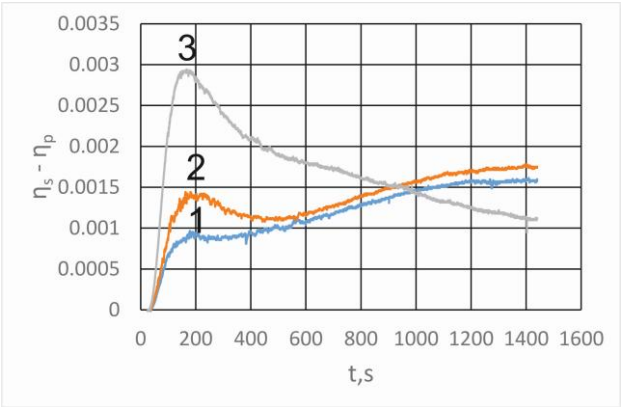

Fig.11. DA difference versus time in the case of *L-R* recording. Reflection mode.

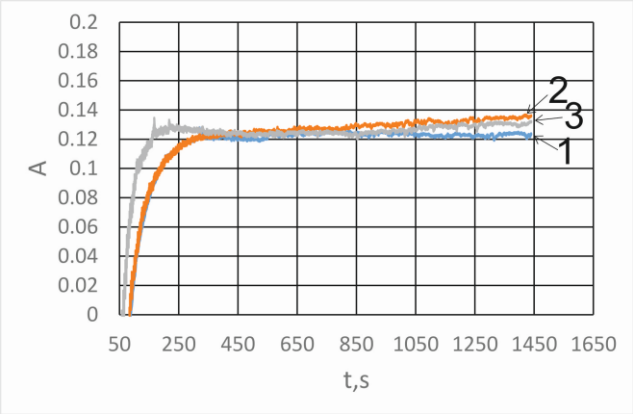

Fig.12. PA contrast versus time in the case of *p-p* recording. Transmission mode.

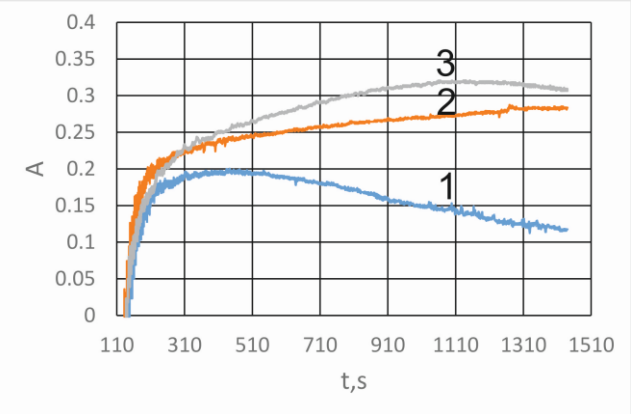

Fig.13. PA contrast versus time in the case of *p-p* recording. Reflection mode.

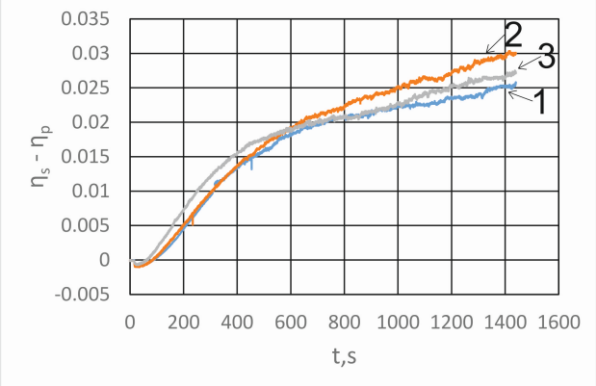

Fig.14. DE difference versus time in the case of *p-p* recording. Transmission mode.

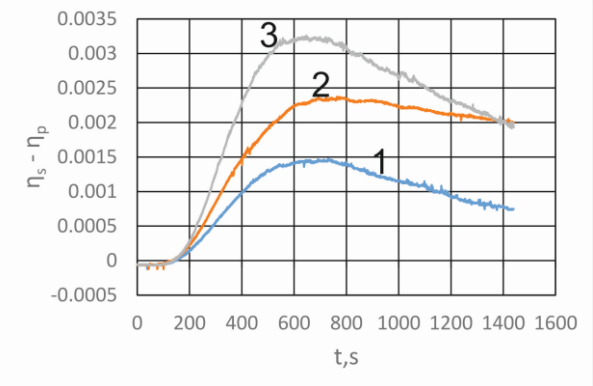

Fig.15. DA difference versus time in the case of *p-p* recording. Reflection mode.

As seen from anisotropy contrast exposure time dependences (Figs. 4, 5, 8, 9, 12 ,13), a specific feature of PA in IWK-2D film is that very fast *A* changes take place at the beginning of exposure.

More accurate studies have shown that they were not measurement artifacts. Rather, very fast initial PA changes took place unresolved by our LPM. These and other experimental results are discussed in the next section.

Experimental measurements are quantitatively summarized in Tables 1 and 2 where maximal DE values at *s*- and *p*- polarizations as well as corresponding specific recording energies and anisotropy contrasts are shown for each recording polarization pair.

Table 1. Holographic and PA parameters in the transmission mode

Recording polarizations	η_s [%]	W_s [J/cm^2%]	η_p [%]	W_p [J/cm^2%]	A	η_s - η_p
L-L	6.6	81	5.1	106	0.19	0.017
L-R	11.8	45	7.3	72	0.23	0.045
p-p	12.6	42	9.6	55	0.12	0.030

Table 2. Holographic and PA parameters in the reflection mode

Recording polarizations	η_s [%]	W_s [J/cm^2%]	η_p [%]	W_p [J/cm^2%]	A	η_s - η_p
L-L	0.42	133	0.261	205	0.24	0.0016
L-R	0.80	71	0.52	103	0.20	0.0029
p-p	0.76	275	0.43	485	0.32	0.0032

Maximal surface relief changes measured by AFM ("RENISHAW in Via Raman Microscope") after the exposure are shown in Table 3.

Table 3. Maximal surface relief changes

	L-L	*L-R*	*p-p*
Δd [nm]	400	1000	150

Practically no changes in Raman spectra before and after the recording were found.

It can be seen from the Tables 1-3 that recording efficiency was maximal for *p-p* recording polarizations in transmission mode, and for *L-R* recording polarizations in reflection mode. Also, recording efficiency did not correlate with PA. The same conclusion we have made also previously for other materials [7].

Discussion

IWK-2D films consists of push-pull molecules shown in Fig.1 bound together by van der Waals forces. They are azobenzene push-pull chromophores with dialkylamino electron donating fragments and dicyanomethylene electron acceptor groups. Bulky triphenyl functional groups are added to avoid crystallization. Under the influence of 532 nm polarized light charge transfer from donors to acceptors take place through aromatic core bridge enabling reorientation of a molecule perpendicularly to the electric field of light because the photoinduced transition probability is proportional to the scalar product of transition dipole moment and light electric field vectors [8]. These photoorientations of chromophores are followed by cyclic *trans-cis-trans* photoisomerization and mass transfer [2,4,6] leading to photoinduced birefringence (PIB) and PA. This follows from the fact that anisotropy contrast calculated by Kogelnik's theory [9] for scalar amplitude-phase transmission gratings (A=0.022) is much smaller than observed (Tables 1,2). Global optical axis perpendicular to the surface arises in the case of *L-L* recording polarizations, and parallel to the surface in the case of *p-p* polarizations, whereas local optical axes with varying orientation arise in the case of *L-R* polarizations.

Initially, surface relief gratings (SRG) dominated both on transmission and reflection because the effective thickness $d_{eff} = 1/\alpha$ =0.25 μm of volume transmission gratings (VTG) was much smaller than the film thickness of 3 μm. Further, in the course of exposure the role of VTG on transmission increased because of observed photobleaching. This conclusion is confirmed by

calculations of SRG contributions to transmission DE at the end of exposure using the data of Table 3 and the formulae presented in [10]: 30%, 66% and 2.4% in the *L-L*, *L-R* and *p-p* cases, respectively. As for reflection, DE is almost completely determined by SRG [11]. From the diffraction grating theory it follows that $\eta_s > \eta_p$ both for VTG and SRG [11, 12] as observed. The exception is the very beginning of exposure when fast *A* oscillations and $\eta_s < \eta_p$ values took place (Figs. 4-15), probably, due to the elastooptic and photodichroic effects. As for SRG, we believe that photoisomerization mechanism [4] plays the main role because it explains the higher Δd values for circular recording polarizations (Table 3).

Summary

PA is studied by holographic method in IWK-2D molecular glassy film for three recording beam polarizations. Transmission mode PA is determined by both SRG and PIB through VTG whereas reflection mode PA is determined by SRG. The obtained results are quite different compared to previously studied K-D-24, K-D-25, K-D-32 and a-As_2S_3 films. Besides, PA details depend also on recording beam polarizations.

Acknowledgement

The financial support of Latvian State Programme "Multifunctional materials and composites, photonics and nanotechnologies. Project 1: Photonics and materials for photonics" (IMIS2) is greatly acknowledged.

References

[1] F. Weigert, Über einen neuen Effekt der Strahlung in lichtsempfindlichen Schichten, Verh. Deutsch. Phys. 21 (1919) 479-483.

[2] G.J.Fang, J.E.Maclennan, Y.Yi, M.A.Glaser, M.Farrow, E.Korblova, D.M.Walba, T.E.Furtak, and N.A.Clark, Athermal photofluidization of glass, Nature Communications 4:152 (2013)1-10, DOI:10.1038/ncommuns2483.

[3] Sam-Shajing Sun and Larry R.Dalton (editors), Introduction to Organic and Optoelectronic Materials and Devices, CRC Press, Taylor and Francis Group, Boca Raton, London, NY, 2008.

[4] Yue Zhao and Tomiki Ikeda (editors), Smart Light-Responsive Materials. Azobenzene-Containing Polymers and Liquid Crystals, A John Wiley&Sons, Inc., Hoboken, New Jersey, 2009.

[5] A.Ozols, V.Kokars, P.Augustovs, I.Uiska, K.Traskovskis, and Dm. Saharov, Effect of light polarization on holographic recording in glassy azocompounds and chalcogenides. Centr. European J.Phys., 9 (2011) 547-552. DOI: 10.2478/s11534-010-0125-6.

[6] A.Jacquart, E.Morin, F.Yang, B.Geffroy, and E.Ishow, Influence of extrinsic and intrinsic parameters onto the formation of surface relief gratings in polar azo molecular glasses, Dyes and Pigments, 92 (2012) 790-797.

[7] A.Ozols, V.Kokars, P.Augustovs, K.Traskovskis, D.Saharov. Holographic studies of photoinduced anisotropy in molecular glassy films containing diphenylamine azochromophores, IOP Conf.Series:Materials Science and Engineering, 38 012011 (2012), 1-6.

[8] D.I.Blohintsev, Foundations of Quantum Mechanics, Nauka, Moscow, 1976 (in Russian).

[9] H.Kogelnik, Coupled wave theory for thick hologram gratings, 48 (1969) 2909-2947.

[10] A.Ozols, M.Reinfelde, Dm.Saharov, K.Kundzins, V.Kampars, and V.Kokars, Holographic recording of surface relief gratings in tolyle-based azobenzene oligomers, Thin Solid Films, 516 (2008) 8887-8892.

[11] T.K.Gaylord and M.G.Moharam, Analysis and applications of optical diffraction by gratings, Proc. of the IEEE, 73 (1985) 894-937.

[12] M.C.Gupta and S.T.Peng, Diffraction characteristics of surface-relief gratings, Applied Optics 32 (1993) 2911-2917.